2013 American Control Conference (ACC)
Washington, DC, USA, June 17-19, 2013

Data-based Modeling of a Lithium Iron Phosphate Battery as an Energy Storage and Delivery System

Xin Zhao and Raymond A. de Callafon

Abstract— **Lithium-ion batteries are important for storage and delivery of electrical energy. Monitoring and prediction of the dynamic and time-dependent effects of lithium-ion batteries is crucial in a battery management system (BMS). In this paper, a dynamic model for the battery as an energy storage and delivery system is proposed. The structure and the parameters of the battery models are estimated by monitoring a charge/discharge demand signal and a power storage/delivery signal in real time. The model is combined by individual linear dynamic models, where the parameters can be estimated by a least-squares algorithm and implemented in a recursive fashion. Based on data obtained from the experimental setup, the dynamic model is applied to predict the dynamics of the energy storage and delivery, and validated against real-time measurements. The results show that the model can capture and predict the dynamics of the energy storage and delivery of the battery, which can benefit the control of lithium-ion batteries.**

I. Introduction

Lithium-ion batteries are considered as one of the primary candidates for electric energy storage for the next generation of automotive and aerospace applications. Since energy generated is hardly equal to the energy consumed at a given time in an energy transmission system, energy storage is needed to buffer gaps in energy delivery. Lithium-ion batteries as electrochemical storage devices also provide energy buffering in smart grids, since they provide one of the best energy densities, exhibit no memory effect, and have low self-discharge when not in use [1–3].

In high-power demand applications, lithium-ion batteries may suffer thermal runaway and cell rupture if overcharged [4]. In extreme cases the overcharge can lead to combustion. Deep discharge may cause the crystalline morphology transition, which can adversely affect the cyclability [1], namely, the life of the lithium-ion battery is shortened. Hence, in most practical applications, the lithium-ion batteries should be monitored and controlled by a BMS, which is a system composed of hardware and software. The main function of a BMS is to control the charging and discharging of the battery while guaranteeing reliable and safe operation [5]. A dynamic battery model is necessary to design the BMS control algorithms. The dynamic model should capture the dynamics of the power storage and delivery of the battery.

A conventional BMS uses an equivalent circuit model, which is derived from the electric characteristics of the battery. A typical equivalent circuit model is composed by equivalent potential, internal resistance, and effective capacitance, which is suitable for portable power system studies [6]. Though some equivalent circuit models are intended to describe the electrochemical characteristics of the battery [7, 8], they still have limited prediction capability compared to physics-based electrochemical models [9].

The electrochemical models of lithium-ion batteries have been studied for decades and they are typically a system of nonlinear partial differential equations. The electrochemical models present a detailed description of the internal physical and chemical processes of lithium-ion batteries [9–13]. However, an exact electrochemical model cannot be used in control applications due to constraints on model complexity for embedded systems in real-time battery monitoring. Approximation of the electrochemical model can be done via a single particle model (SPM) [14]. Due to the constrained assumption, the SPM is of limited use in practice, especially in the case of high-current operations [9]. Compared with the equivalent circuit models, the parameters of an electrochemical model have a physical interpretation, but the amount of parameters is usually too large to be estimated efficiently [15]. Novel approaches in PDE estimation can reduce the number of parameters to be estimated [12, 13], but still may have the inherent assumption of full state measurements to allow parameter estimation. Instead of focusing on the dynamics of the electrochemical process of the battery, it is important to model the dynamics of the energy storage capacity of the battery as a function of energy demand based on measurable input/output signals in real time.

The purpose of this paper is to show how a lithium-ion battery can be modelled as a dynamic model for energy storage. As such, we are interested in modeling how fast a battery can store and deliver energy as a function of time. The proposed model is a different approach from the traditional equivalent circuit models [6–8] or electrochemical models [9–17], as we are not modeling the current-voltage dynamics, but the power delivery dynamics. As indicated in Fig. 1, this is done with a parameter estimation method that models the individual dynamics from a power charge/discharge demand signal to the voltage and the current signals of a lithium iron phosphate ($LiFePO_4$) battery. The models are combined to formulate a dynamic model of a battery as a power storage and delivery system.

The $LiFePO_4$ batteries are less expensive and less toxic than other lithium-ion batteries, such as lithium cobalt oxide ($LiCoO_2$) batteries. Additionally, the $LiFePO_4$ battery can provide high energy storage capacity and high discharge

Xin Zhao is with the Department of Mechanical and Aerospace Engineering, University of California San Diego, 9500 Gilman Drive, Mail Code 0411, La Jolla, CA 92093-0411, USA xiz028@ucsd.edu

Raymond A. de Callafon is with Faculty of Mechanical and Aerospace Engineering, University of California San Diego, 9500 Gilman Drive, Mail Code 0411, La Jolla, CA 92093-0411, USA callafon@ucsd.edu

978-1-4799-0176-0/$31.00 ©2013 AACC

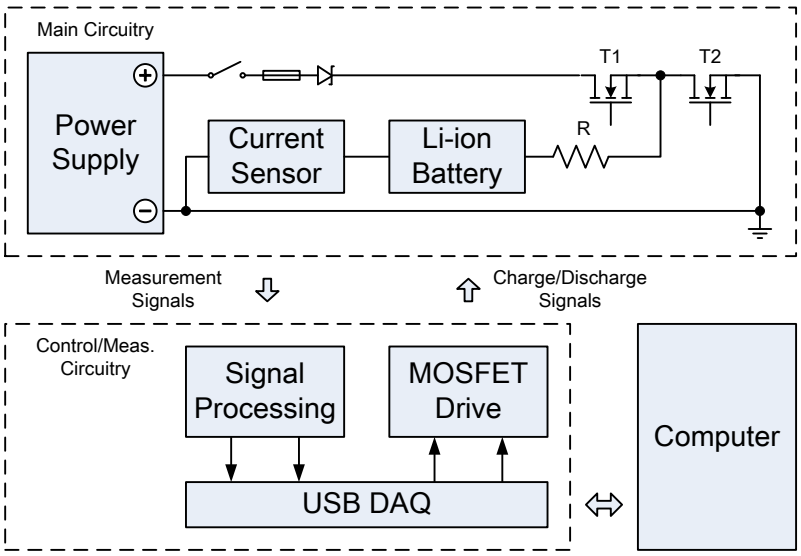

Fig. 2. Schematic of the experimental battery tester with charge/discharge load

power, and it is proved to have a long cycle life and high stability [18]. Therefore, the application of $LiFePO_4$ batteries can further benefit the performance of energy storage systems.

II. Experimental Setup

To model a battery as a power storage and delivery system, an experimental setup is created where a charge/discharge demand signal can be applied while measuring the voltage and the current of the battery in real time. The schematic of the experimental setup is shown in Fig. 2 and can be explained as follows.

In the main circuitry, the charge/discharge cycles are directed by the MOSFETs T_1 and T_2. When T_1 is turned on and T_2 is off, the battery is connected to the power supply and charged. While T_1 is turned off and T_2 is on, the battery is disconnected from the power supply but connected to the ground via the resistance R, thus the battery is discharged. Pulse Width Modulations of T_1 and T_2 allow for modulating charge and discharge demands. The resistance R behaves as a current limiter while the battery is charged, and it is the load when the battery is discharged. The MOSFETs are switched by the corresponding control signals sent from NI-myDAQ. The DAQ device is also employed to acquire the measured signals, and it can communicate with the computer via a USB cable. In the computer, a LabVIEW program is developed to automatically load cycle signals from existing files and save measured signals. Thus the test can be repeated using the same time sequence of charge/discharge demand signals.

In the control and measurement circuitry, a MOSFET drive circuitry is implemented to boost the level of digital output signals from the DAQ. Several low-order Butterworth low-pass filtering circuitries are reserved to process the measured signals for aliasing effects if applicable.

The description of the experimental setup is completed by a photograph of the experimental battery tester depicted in Fig. 3. The battery utilized in the test is a 2.3Ah - 3.3V $LiFePO_4$ battery cell ANR26650 manufactured by A123 Systems. The maximum continuous discharge current of the cell is 70A. The pulse discharge current can be 120A. Hence the cell is suitable for transient high-power applications. Furthermore, the MOSFETs are power MOSFET IRLZ34. A bidirectional $\pm$20A Hall effect sensor ACS714, the sensitivity of which is 100mV/A, is utilized to measure the current, while the voltage over the battery is measured directly via an A/D conversion.

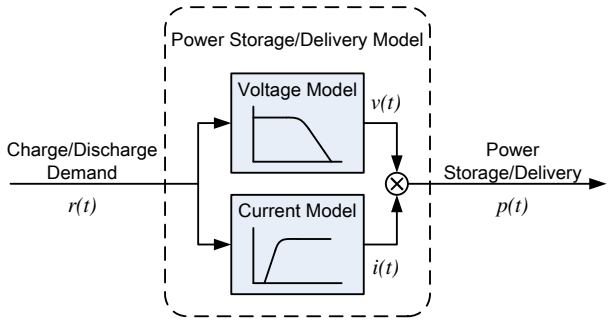

Fig. 1. Diagram of the power storage/delivery model

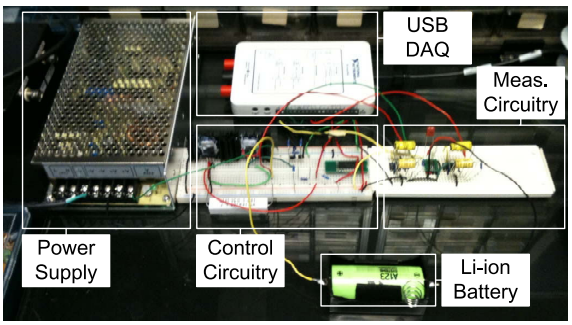

Fig. 3. Photograph of the experimental battery tester

III. Data-based Modeling

In building a dynamic model of a battery as a power storage and delivery system, the power charge/discharge demand signal $r(t)$ acts as an input signal, while the voltage signal $v(t)$ and the current signal $i(t)$ of the battery act as observable output signals. Multiplication of output signals leads to a power storage/delivery signal $p(t)$, as indicated earlier in Fig. 1.

The dynamic model from $r(t)$ to $p(t)$ is possibly nonlinear. But it will be shown in this paper that the separate dynamic models between $r(t)$ as input and $v(t)$ and $i(t)$ as output individually can be modelled fairly well with linear models. The estimation of the separate models is done by linear models with an Auto-Regression with eXogeneous input (ARX) model structure [19]. Compared with other model structures, ARX model can capture the dynamic response of a system to both the input and the noise, and it can be optimized by a relatively simple linear method, which is essentially crucial for the practical application. For ARX models, one can then estimate the parameters by a least-squares method and facilitate the use of a recursive implementation for real-time parameter estimation.

The procedure of building the ARX models between $r(t)$ and $v(t)$ or $i(t)$ is the same. For brevity, we only present the data-based modeling procedure for the voltage model with the input $r(t)$ and the output $v(t)$. Specifically, the voltage model is in the form

$$v(t) = \frac{B(q,\theta)}{A(q,\theta)} r(t) + \frac{1}{A(q,\theta)} \varepsilon(t,\theta) \tag{1}$$

where

$$\begin{aligned} A(q,\theta) &= 1 + a_1 q^{-1} + \cdots + a_{n_a} q^{-n_a} \\ B(q,\theta) &= b_1 q^{-1} + \cdots + b_{n_b} q^{-n_b} \end{aligned}$$

in which q is forward time-shift: $qr(t) = r(t+1)$ and the parameter vector

$$\theta = \begin{bmatrix} a_1 & \cdots & a_{n_a} & b_1 & \cdots & b_{n_b} \end{bmatrix}^T \tag{2}$$

captures the unknown coefficients in the $A(q,\theta)$ and $B(q,\theta)$ polynomials.

To estimate the parameters, the error $\varepsilon(t,\theta)$ is written in a linear regression form

$$\varepsilon(t,\theta) = \varphi^T(t)\theta \tag{3}$$

where the regression vector

$$\begin{aligned} \varphi(t) = [&-v(t-1) \quad \cdots \quad -v(t-n_a) \\ &r(t-1) \quad \cdots \quad r(t-n_b)]^T \end{aligned} \tag{4}$$

consists of past voltage measurements $v(s),\ \ s < t$ and past charge/discharge demand signal $r(s),\ \ s < t$. We assume an inherent one-step time delay between the voltage and the charge/dischrage demand signal.

Due to the linear regression, the parameters can be estimated by the least-squares method, which minimizes the least-squares criterion

$$V_N(\theta, Z^N) = \frac{1}{N} \sum_{t=1}^{N} \frac{1}{2} [v(t) - \varphi^T(t)\theta]^2 \tag{5}$$

The criterion can be minimized analytically, which gives the least-squares estimate (LSE) [19]

$$\hat{\theta}_N^{LS} = \arg\min V_N(\theta, Z^N) = R^{-1}(N) \cdot f(N) \tag{6}$$

provided the inverse of $R(N)$ exists, where

$$R(N) = \frac{1}{N} \sum_{t=1}^{N} \varphi(t)\varphi^T(t), \quad f(N) = \frac{1}{N} \sum_{t=1}^{N} \varphi(t) v(t)$$

To quantify the output variation that is explained by the model, the k-step-ahead predictor $\hat{v}(t|t-k)$ is introduced as

$$\hat{v}(t|t-k) = W_k(q)G(q)r(t) + [1 - W_k(q)]v(t) \tag{7}$$

$$W_k(q) \triangleq \bar{H}_k(q)H^{-1}(q), \quad \bar{H}_k(q) = \sum_{l=0}^{k-1} h(l) q^{-l} \tag{8}$$

where $h(l)$ is the impulse response of $H(q)$. For an ARX model, the filters $G(q,\theta)$ and $H(q,\theta)$ are parametrized as

$$G(q,\theta) = \frac{B(q,\theta)}{A(q,\theta)}, \quad H(q,\theta) = \frac{1}{A(q,\theta)} \tag{9}$$

Substituting (8) and (9) into (7), then the k-step-ahead predictor can be rewritten as (omitting the parameter θ dependency for brevity)

$$\hat{v}(t|t-k) = \bar{H}_k(q)B(q)r(t) + [1 - \bar{H}_k(q)A(q)]v(t) \tag{10}$$

Finally, the model fit ratio is introduced:

$$\alpha_v = (1 - \frac{\|\hat{v}(t|t-k) - v\|}{\|v - \bar{v}\|}) \times 100\% \tag{11}$$

where $\bar{v}$ is the mean value of output.

Following the same procedure, we can also get the estimated parameters $\hat{\theta}_N^{LS}$ for the current model and the k-step-ahead predictor $\hat{i}(t|t-k)$. Then we can define the k-step-ahead predictor for the power storage and delivery model as

$$\hat{p}(t|t-k) = \hat{v}(t|t-k) \cdot \hat{i}(t|t-k) \tag{12}$$

Thus we can also get the model fit ratios α_i and α_p to quantify the prediction ability of the model.

In practice, if the number of data is large enough, then the data can be separated into two sets, which are for estimation and validation respectively. Furthermore, a few tests are taken to estimate the model order. With the model order increases, there exists one that can achieve the best model fit. If the model performance does not improve at higher orders, low-order models might fit the data equally well. The process of determining the model order can be taken iteratively.

IV. Recursive Implementation

Recursive estimation of the parameter estimate $\hat{\theta}_t^{LS}$ as a function of time t allows real-time monitoring of the energy storage dynamics of the battery. Instead of batch-wise estimation using N data points to obtain $\hat{\theta}_N^{LS}$ given in (6), we compute the parameter estimate as the data from the power demand signal $r(t)$, the voltage $v(t)$ and the current $i(t)$ are measured.

To formulate a computational effective recursive estimation for $\hat{\theta}_t^{LS}$, with

$$R(t) = \frac{1}{t}\sum_{\tau=1}^{t}\varphi(\tau)\varphi^T(\tau)$$

we have the relationship between $R(t-1)$ and $R(t)$

$$R(t) = \frac{t-1}{t}R(t-1) + \frac{1}{t}\varphi(t)\varphi^T(t) \tag{13}$$

Note that matrix $R(t)$ is related to the inverse of the *covariance of the parameter estimate* $\hat{\theta}_t$ [19]. Similarly, we can also derive the relationship between $f(t-1)$ and $f(t)$

$$f(t) = \frac{t-1}{t}f(t-1) + \frac{1}{t}\varphi(t)y(t) \tag{14}$$

Then with $\hat{\theta}_t^{LS} = R^{-1}(t)f(t)$, use the fact that $\hat{\theta}_{t-1}^{LS} = R^{-1}(t-1)f(t-1)$ or $f(t-1) = R(t-1)\hat{\theta}_{t-1}^{LS}$, substitution yields

$$\hat{\theta}_t^{LS} = R^{-1}(t)\left[\frac{t-1}{t}R(t-1)\hat{\theta}_{t-1}^{LS} + \frac{1}{t}\varphi(t)y(t)\right]$$

Finally we use (13) to substitute

$$R(t-1) = \frac{t}{t-1}R(t) - \frac{1}{t-1}\varphi(t)\varphi^T(t)$$

and we obtain

$$\hat{\theta}_t^{LS} = \hat{\theta}_{t-1}^{LS} + \frac{1}{t}R(t)^{-1}\varphi(t)[y(t) - \varphi^T(t)\hat{\theta}_{t-1}^{LS}] \tag{15}$$

If we now define

$$\varepsilon(t, \hat{\theta}_{t-1}^{LS}) = y(t) - \varphi^T(t)\hat{\theta}_{t-1}^{LS} \tag{16}$$

as the *a posteriori* prediction error, we can formulate a recursive parameter update by the order of (16), (13), and (15). In practice, the update of $R(t)$ can also be replaced by the update of the inverse of $R(t)$ and combined with the matrix inversion lemma to improve computational efficiency. Specifically, introduce the covariance matrix

$$P(t) \triangleq [tR(t)]^{-1} = [(t-1)R(t-1) + \varphi(t)\varphi^T(t)]^{-1} \tag{17}$$

Apply the matrix inversion lemma (A.1) to (17). With (13), taking $A = (t-1)R(t-1) = P^{-1}(t-1)$, $B = D^T = \varphi(t)$, and $C = 1$ gives

$$P(t) = P(t-1) - \frac{P(t-1)\varphi(t)\varphi^T(t)P(t-1)}{\varphi^T(t)P(t-1)\varphi(t) + 1} \tag{18}$$

Thus, the recursive parameter update can be formulated by the following three steps:

- *a posteriori* prediction error update

$$\varepsilon(t, \hat{\theta}_{t-1}^{LS}) = y(t) - \varphi^T(t)\hat{\theta}_{t-1}^{LS} \tag{19}$$

- covariance update

$$P(t) = P(t-1) - \frac{P(t-1)\varphi(t)\varphi^T(t)P(t-1)}{\varphi^T(t)P(t-1)\varphi(t) + 1} \tag{20}$$

- parameter update

$$\hat{\theta}_t^{LS} = \hat{\theta}_{t-1}^{LS} + P(t)\varphi(t)\varepsilon(t, \hat{\theta}_{t-1}^{LS}) \tag{21}$$

It should be noted that the above three steps at $t = N$ gives the exact same parameter value $\hat{\theta}_N^{LS}$ as in (6), provided θ_0 and P_0 are initialized correctly, but the result is now written in terms of the previous parameter estimate $\hat{\theta}_{t-1}^{LS}$ in a recursive fashion.

Furthermore we see that

$$\begin{aligned}\lim_{t\to\infty} R(t) &= \lim_{t\to\infty}\frac{1}{t}\sum_{\tau=1}^{t}\varphi(\tau)\varphi^T(\tau) \\ &= \Sigma_{\varphi,\varphi}(0) \text{ w.p. } 1\end{aligned} \tag{22}$$

making $R(t)$ converge to the zero delay auto covariance (matrix) Σ of the regressor $\varphi(t)$ as $t \to \infty$.

Provided $R_{\varphi,\varphi}(0)$ is non-singular, thus

$$\lim_{t\to\infty} P(t) = \lim_{t\to\infty}\frac{1}{t}R^{-1}(t) = 0 \text{ w.p. } 1 \tag{23}$$

which allows the recursive parameter update to *converge to a stationary point* $\theta^\star$ *of the recursion*

$$\lim_{t\to\infty}\hat{\theta}_t^{LS} = \lim_{t\to\infty}\hat{\theta}_{t-1}^{LS} = \theta^\star \text{ w.p. } 1 \tag{24}$$

The convergence is desired when the parameter θ is not changing. However, to account for changes in θ, we adjust the covariance update with the disturbance factor λ to

$$P(t) = P(t-1) - \frac{P(t-1)\varphi(t)\varphi^T(t)P(t-1)}{\varphi^T(t)P(t-1)\varphi(t) + 1} + \lambda I \tag{25}$$

where $0 < \lambda \ll 1$.

With the additional term λI, the convergence w.p. 1 of the parameter estimate is sacrificed to allow parameter adaptation. For a converged estimation, the covariance update $P(t)$ is expected to converge to zero. Therefore, λ must be sufficiently small to ensure the stability of the algorithm.

V. Experimental Results

The charge/discharge cycle shown in Fig. 4 is utilized in the test, where the charge/discharge signal +1 represents full charging and -1 represents full discharging. The cycle is created by a stretched pseudo-random binary signal (PRBS) of order 6. Though the stretching leads to the loss of white-noise-like properties, the sequence still contains all the possibilities of binary combinations of order 6.

The measured signals of voltage and current are also shown in Fig. 4. The sampling rate is 10Hz, since normally the parameters of a battery vary slowly. The signals vary with the alternating between charge and discharge as expected. Due to the design of the circuitry, the charge and discharge current is approximately at the rate of 1C, which is 2.3A. As shown in Fig. 4, the dynamic model of the voltage can be considered as a low-pass filter, while the dynamic model of the current can be treated as a high-pass filter or a gain function.

A. Experimental data-based modeling

For identification and model validation purposes, the data is separated into two sets. The measured data of the first 15 minutes is used to estimate the parameters, and the rest of the data is applied to validate the models. Both a batch-wise

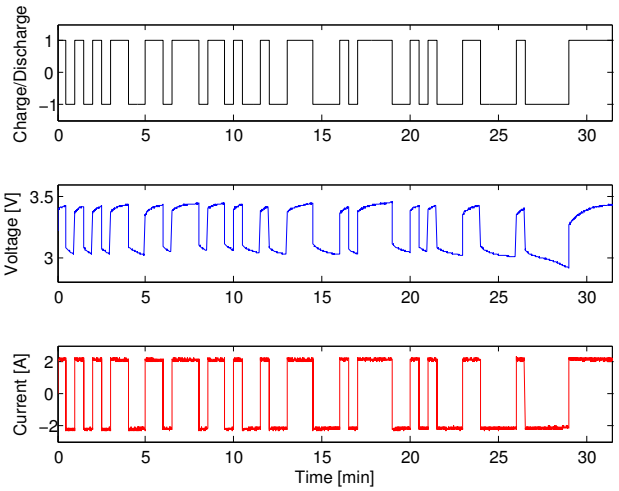

Fig. 4. Experimental results (cycle, voltage, current)

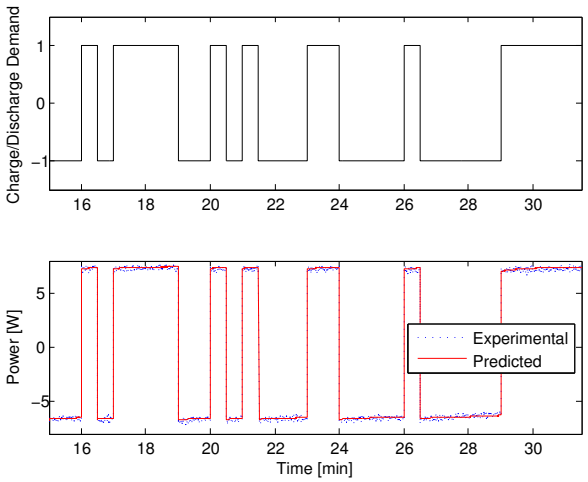

Fig. 6. 5-step-ahead prediction of the power storage/delivery model

estimation and a recursive estimation are used on the first 15 minutes of experimental data. Following the data-based modeling presented in the previous section, the batch-wise estimation leads to the following linear voltage model and the linear current model:

- Voltage Model

$$v(t) = \frac{0.167q^{-1} - 0.08295q^{-2} - 0.08387q^{-3}}{1 - 0.5031q^{-1} - 0.4969q^{-2}} r(t) + \frac{1}{1 - 0.5031q^{-1} - 0.4969q^{-2}} e(t)$$

- Current Model

$$i(t) = \frac{2.09q^{-1}}{1 - 0.03149q^{-1}} r(t) + \frac{1}{1 - 0.03149q^{-1}} e(t)$$

To capture the dynamics of the current and achieve a better model fit, the second-order term of the current model is reserved. A model with more dynamics is expected to be obtained through the tests with varying input in the future.

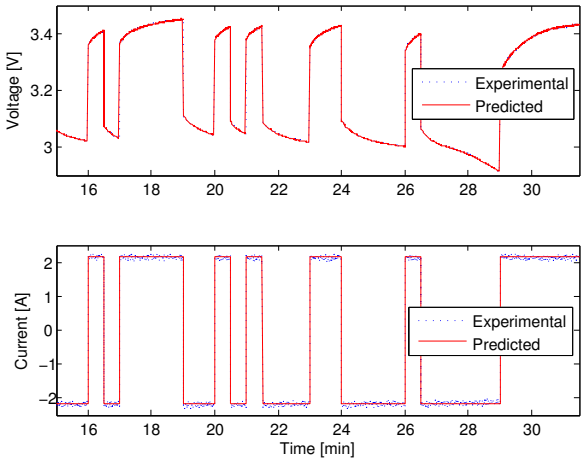

Fig. 5. 5-step-ahead prediction of the voltage and current models

To validate the model, the prediction quality of the model is tested. As mentioned above, the k-step-ahead predictor $\hat{v}(t|t-k)$, $\hat{i}(t|t-k)$, and $\hat{p}(t|t-k)$ is computed from past data, including k-step-ahead outputs and up-to-now inputs. The 5-step-ahead prediction of voltage and current is shown in Fig. 5, in comparison with the measured data. As shown in Fig. 5, the prediction of voltage and current is close to the measured data. The power storage/delivery model is built by combining the two individual dynamic models. The 5-step-ahead prediction of power is shown in Fig. 6. The model fit ratios of the voltage model, the current model, and the power storage/delivery model are shown in Table I.

TABLE I
MODEL FIT RATIOS α

Voltage Model	α_v	99.112%
Current Model	α_i	97.979%
Power Storage/Delivery Model	α_p	97.994%

The estimation results indicate that a fairly simple model created by the multiplication of two linear models in a signal setting from the charge/discharge demand signal $r(t)$ to the power storage and delivery signal $p(t) = v(t) \cdot i(t)$ is able to capture the energy storage dynamics of the battery very well. The model has been validated on data not used during the identification.

B. Recursive implementation of parameter estimate

Applying the recursive parameter update procedure (19), (20), and (21), we can get the recursive estimated parameters of linear voltage and current models shown in Fig. 7. As expected, the estimated parameters indicated as solid lines converge to the parameters estimated by (6) indicated as dashed lines. Hence the recursive implementation can also estimate the parameters of the required linear models of voltage and current.

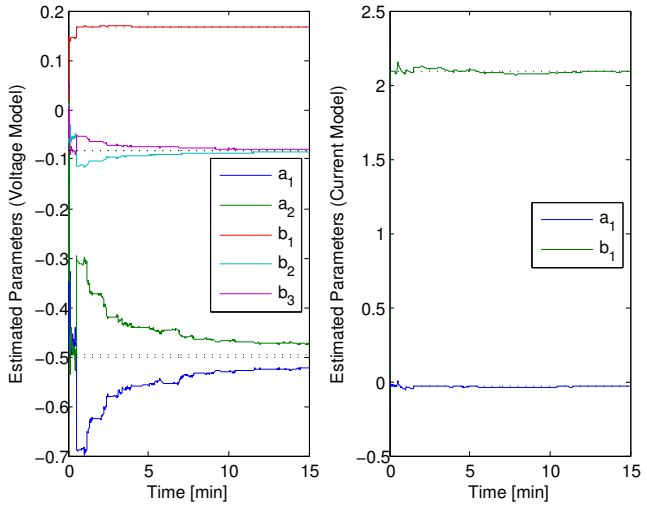

Fig. 7. Estimated parameters of voltage and current models ($\lambda = 0$)

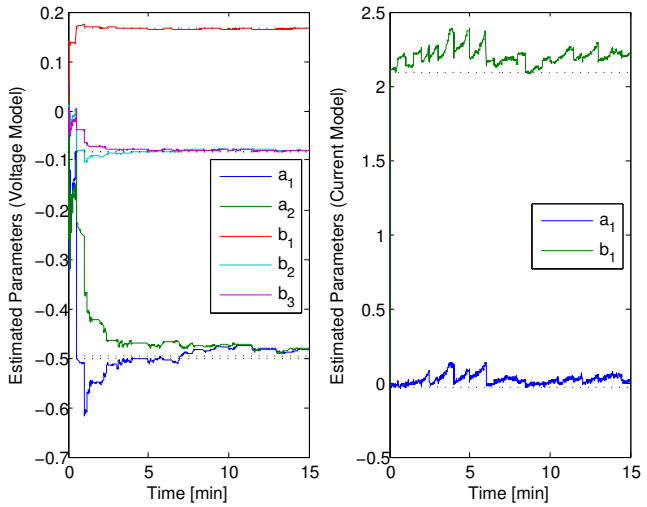

Fig. 8. Estimated parameters of voltage and current models ($\lambda = 0.005$)

When the disturbance factor λ is non-zero, the recursive estimated parameters do not converge but become more sensitive to the latest measured signals as shown in Fig. 8.

VI. Conclusions & Future Work

A dynamic model of the $LiFePO_4$ battery as an energy storage and delivery system is formulated in this paper. This is done by two separate linear dynamic models from a charge/discharge demand signal to the voltage and current signals measured at the battery in real time. Multiplication of both dynamic models yields the dynamic model that accurately models the dynamics from the demand signal to the power storage/delivery signal of the battery. Based on experimental data obtained from a battery test setup, parameters of the dynamic model are estimated in batch and recursively. Comparison of simulated and measured data validates the proposed dynamic model.

For further work on building the dynamic battery model, the test circuitry can be modified to adopt pulse width modulated charge/discharge demand signals. Long-term tests can be taken into account via recursive estimation to assist in the management of the battery as part of a larger energy storage and delivery system.

Appendix

- Matrix Inversion Lemma

$$[A+BCD]^{-1} = A^{-1} - A^{-1}B[DA^{-1}B+C^{-1}]^{-1}DA^{-1} \quad \text{(A.1)}$$

References

[1] Y. Nishi, "Lithium ion secondary batteries: past 10 years and the future," *Journal of Power Resource*, vol. 100, pp. 101–106, 2001.

[2] J.-M. Tarascon and M. Armand, "Issues and challenges facing rechargeable lithium batteries," *Nature*, vol. 414, pp. 359–367, 2001.

[3] M. Armand and J.-M. Taracson, "Building better batteries," *Nature*, vol. 451, pp. 652–657, 2008.

[4] R. Spotnitz and J. Franklin, "Abuse behavior of high-power, lithium-ion cells," *Journal of Power Resource*, vol. 113, pp. 81–100, 2003.

[5] T. Stuart, F. Fang, X. Wang, C. Ashtiani, and A. Pesaran, "A modular battery management system for HEVs," in *Proceedings of the SAE Future Car Congress*, no. 2002-01-1918, 2002.

[6] L. Gao, S. Liu, and R. A. Dougal, "Dynamic lithium-ion battery model for system simulation," *IEEE Transactions on Components and Packing Technologies*, vol. 25, no. 3, pp. 495–505, September 2002.

[7] J. Lee, O. Nam, and B. H. Cho, "Li-ion battery soc estimation method based on the reduced order extended kalman filtering," *Journal of Power Resource*, vol. 174, pp. 9–15, 2007.

[8] M. W. Verbrugge and P. Liu, "Electrochemical characterization of high-power lithium ion batteries using triangular voltage and current excitation sources," *Journal of Power Resource*, vol. 174, pp. 2–8, 2007.

[9] N. A. Chaturvedi, R. Klein, J. Christensen, J. Ahmed, and A. Kojic, "Algorithms for advanced battery-management systems," *IEEE Control Systems*, vol. 30, pp. 49–68, June 2010.

[10] M. Doyle, T. F. Fuller, and J. Newman, "Modeling of galvanostatic charge and discharge of the lithium/polymer/insertion cell," *Journal of Electrochemical Society*, vol. 140, pp. 1526–1533, June 1993.

[11] T. F. Fuller, M. Doyle, and J. Newman, "Simulation and optimization of the dual lithium ion insertion cell," *Journal of Electrochemical Society*, vol. 141, pp. 1–10, January 1994.

[12] S. J. Moura, N. A. Chaturvedi, and M. Krstic, "PDE estimation techniques for advanced battery management systems - Part I: SOC estimation," in *Proceedings of the 2012 American Control Conference*, Montreal, Canada, 2012, pp. 559–565.

[13] ——, "PDE estimation techniques for advanced battery management systems - Part II: SOH identification," in *Proceedings of the 2012 American Control Conference*, Montreal, Canada, 2012, pp. 566–571.

[14] S. Santhanagopalan and R. E. White, "Online estimation of the state of charge of a lithium ion cell," *Journal of Power Resource*, vol. 161, pp. 1346–1355, 2006.

[15] J. C. Forman, S. J. Moura, J. L. Stein, and H. K. Fathy, "Genetic parameter identification of the doyle-fuller-newman model from experimental cycling of a $LiFePO_4$ battery," in *Proceedings of the 2011 American Control Conference*, San Francisco, USA, 2011, pp. 362–369.

[16] D. Domenico, G. Fiengo, and A. Stefanopoulou, "Lithium-ion battery State of Charge estimation with a Kalman filter based on a electrochemical model," in *Proceedings of the 17th IEEE International Conference on Control Applications*, San Antonio, USA, 2008, pp. 702–707.

[17] R. Klein, N. Chaturvedi, J. Christensen, J. Ahmed, R. Findeisen, and A. Kojic, "Electrochemical model based observer design for a lithium-ion battery," *IEEE Transaction on Control Systems Technology*, vol. 21, pp. 289–301, 2013.

[18] S. Yang, Y. Song, P. Y. Zavalij, and M. S. Whittingham, "Reactivity, stability and electrochemical behavior of lithium iron phosphates," *Electrochemistry Communications*, vol. 4, pp. 239–244, 2002.

[19] L. Ljung, *System Identification: Theory for the User*. Prentice Hall PTR, 1999.